HHS Public Access

Author manuscript

Nat Immunol. Author manuscript; available in PMC 2018 January 23.

Published in final edited form as:

Nat Immunol. 2016 April ; 17(4): 422–432. doi:10.1038/ni.3410.

A molecular threshold for effector CD8+ T cell differentiation controlled by transcription factors Blimp-1 and T-bet

Annie Xin[1,2,9], **Frederick Masson**[1,2,8,9], **Yang Liao**[1,2], **Simon Preston**[1,2], **Tianxia Guan**[3], **Renee Gloury**[1,2], **Moshe Olshansky**[1,4], **Jian-Xin Lin**[5], **Peng Li**[5], **Terence P Speed**[1,6], **Gordon K Smyth**[1,6], **Matthias Ernst**[1,2,8], **Warren J Leonard**[5], **Marc Pellegrini**[1,2], **Susan M Kaech**[4,7], **Stephen L Nutt**[1,2], **Wei Shi**[1,6], **Gabrielle T Belz**[1,2], and **Axel Kallies**[1,2]

[1]The Walter and Eliza Hall Institute of Medical Research, Parkville, Victoria, Australia

[2]The Department of Medical Biology, University of Melbourne, Parkville, Victoria, Australia

[3]Department of Immunobiology, Yale University School of Medicine, New Haven, Connecticut, USA

[4]The Department of Computing and Information Systems, University of Melbourne, Parkville, Victoria, Australia

[5]Laboratory of Molecular Immunology and Immunology Center, National Heart, Lung, and Blood Institute, National Institutes of Health, Bethesda, Maryland, USA

[6]The Department of Mathematics and Statistics, University of Melbourne, Parkville, Victoria, Australia

[7]Howard Hughes Medical Institute, Chevy Chase, Maryland, USA

Abstract

T cell responses are guided by cytokines that induce transcriptional regulators, which ultimately control differentiation of effector and memory T cells. However, it is unknown how the activities of these molecular regulators are coordinated and integrated during the differentiation process. Using genetic approaches and transcriptional profiling of antigen-specific CD8+ T cells, we reveal a common program of effector differentiation that is regulated by IL-2 and IL-12 signaling and the combined activities of the transcriptional regulators Blimp-1 and T-bet. The loss of both T-bet and

Correspondence should be addressed to A.K. (kallies@wehi.edu.au).

[8]Present address: Olivia Newton-John Cancer Research Institute and La Trobe University School of Cancer Medicine, Heidelberg, Victoria, Australia.

[9]These authors contributed equally to this work.

Accession codes. Gene Expression Omnibus: RNA sequencing data have been deposited under accession code GSE68056.

Note: Any Supplementary Information and Source Data files are available in the online version of the paper.

AUTHOR CONTRIBUTIONS

A.X. and F.M. planned and performed most experiments; S.P., R.G. and T.G. performed additional experiments; Y.L., W.S. and G.K.S. analyzed most RNA and ChIP sequencing experiments; M.O., J.-X.L., P.L. and T.P.S. contributed to the RNA sequencing analysis; M.E., W.J.L., S.M.K. and M.P. contributed to the scientific planning and organization of experiments; S.L.N., G.T.B. and A.K. conceived the idea for the study and designed experiments; A.K. oversaw and designed the study; A.X., F.M. and A.K. wrote the manuscript.

COMPETING FINANCIAL INTERESTS

The authors declare no competing financial interests.

Blimp-1 leads to abrogated cytotoxic function and ectopic IL-17 production in $CD8^+$ T cells. Overall, our data reveal two major overlapping pathways of effector differentiation governed by the availability of Blimp-1 and T-bet and suggest a model for cytokine-induced transcriptional changes that combine, quantitatively and qualitatively, to promote robust effector $CD8^+$ T cell differentiation.

T cell responses are directed by multiple cell-extrinsic cues, including antigen, costimulation and cytokines, which induce a molecular network that controls antigen-induced $CD8^+$ T cell differentiation[1–3]. Key aspects of this process have been identified, including the distinct transcriptional profiles of effector and memory T cells[4–6], the impact of T cell antigen receptor (TCR) signaling[7,8], the epigenetic landscape[9] and the temporal organization of $CD8^+$ T cell responses[10].

Cytokines, in particular those that signal through the common γ-chain, such as interleukin 2 (IL-2), or mediate inflammation, such as IL-12, are critical for T cell differentiation[11–15]. Strong or extended IL-2 signaling drives $CD8^+$ T cells to differentiate into effector cells, whereas weak or limited IL-2 signaling promotes their development into memory cells[16,17]. IL-2 induces the expression of the transcription factor Blimp-1 (refs. [17–21]), which in turn drives terminal differentiation of effector T cells and regulates a number of key molecules involved in $CD8^+$ T cell function[22–25]. Conversely, IL-2 also contributes to the programming of $CD8^+$ memory T cells[26,27]. This may be due to the capacity of IL-2 to induce the T-box transcription factor Eomesodermin (Eomes), which is crucial for the development of memory T cells[17,28,29]. Therefore, the biology of IL-2 is complex, and its contribution to effector and memory differentiation is incompletely known. IL-12 has a crucial role in $CD8^+$ T cell responses by inducing T-bet, another T-box transcription factor, which is of central importance for $CD8^+$ effector differentiation and function[5,28,30]. In addition, both IL-2 and IL-12 promote effector differentiation through inducing the expression of transcriptional regulator Id2 (refs. [31–34]). Importantly, this process is balanced by a number of transcription factors, including Eomes, Id3, Bcl-6 and Tcf1, that counteract terminal differentiation and promote development of memory T cells[1–3,33–38]. Thus, cytokines regulate the coordinated and dynamic expression of multiple transcription factors that control the development of cytotoxic effector and memory T cells.

Peripheral $CD8^+$ T cell differentiation in response to infection gives rise to distinct populations of antigen-specific cells, including short-lived effector cells (SLECs) and memory-precursor cells (MPCs)[4,5]. SLECs express high amounts of cytotoxic molecules and cytokines and are considered best equipped to eradicate virus-infected cells. SLEC formation seems particularly susceptible to alterations in the transcriptional repertoire of $CD8^+$ T cells, as deficiencies in transcriptional regulators such as T-bet, Blimp-1 and Id2 lead to severe impairments in SLEC differentiation while leaving MPC development intact[5,24,25,32–34]. This requirement for SLEC differentiation may be due to a tight interdependency of the expression of these transcription factors[24,25,39,40]. In an alternative and not necessarily mutually exclusive model, all three factors—Blimp-1, T-bet and Id2—may regulate the expression of distinct sets of genes critical for SLEC differentiation or contribute to the expression of a common set of genes required for SLEC development.

Although SLEC differentiation is severely impaired in T cells lacking T-bet, Blimp-1, Id2 or IL-2 signaling, $CD8^+$ T cell–mediated viral control is largely preserved[17,25,39,41,42]. This indicates significant robustness in the molecular network regulating T cell function and suggests the existence of mechanisms that preserve effector functions in environments that may be limited by a paucity of inflammatory cytokines or mutations that cripple aspects of T cell function. It remains unknown how the activities of multiple cytokines and transcription factors are integrated to ensure effector function under various physiological conditions.

Here we use broad transcriptional profiling of antigen-specific $CD8^+$ T cells to dissect the relative contributions and interdependency of cytokines and Blimp-1 and T-bet, two major drivers of effector $CD8^+$ T cell differentiation. We show that signals from IL-2 and proinflammatory cytokines, in particular IL-12, combine to induce the expression of graded amounts of Blimp-1 and T-bet, which together in a partially redundant manner control the expression of molecules required for effector and memory T cell differentiation and repress the development of IL-17–producing $CD8^+$ T cells. Consequently, combined deficiency in Blimp-1 and T-bet resulted in an inability to control systemic viral infection and severe immune pathology. These data uncover remarkable robustness in the molecular network governing T cell function and suggest a combinatorial threshold model in which Blimp-1 and T-bet contribute to the expression of overlapping and distinct sets of genes required for the differentiation of effector T cells.

RESULTS

IL-2 is not essential for Blimp-1 expression in $CD8^+$ T cells

To examine whether IL-2 is necessary for Blimp-1 expression *in vivo*, we generated mice that are deficient in IL-2 receptor-α (IL-2Rα) and carry a reporter allele expressing GFP from the *Blimp1* locus (*Il2ra*$^{-/-}$*Blimp1*^{GFP}). We then reconstituted the hematopoietic systems of lethally irradiated congenically marked ($Ly5.1^+Ly5.2^+$) mice with a mix of bone marrow cells from *Il2ra*$^{-/-}$*Blimp1*^{GFP} ($Ly5.2^+$) and *Il2ra*$^{+/+}$*Blimp1*^{GFP} (Ly5.1) mice (Supplementary Fig. 1a). The resulting chimeric mice were primed with a heterologous influenza virus (PR8) then infected with influenza virus HKx31. At the peak of the response, we analyzed antigen-specific $CD8^+$ T cells using tetrameric complexes (Fig. 1a and Supplementary Fig. 1b). Consistent with a role for IL-2 in Blimp-1 induction, splenic IL-2Rα–deficient antigen-specific $CD8^+$ T cells did not differentiate into $KLRG1^+IL\text{-}7R^-$ SLECs (Fig. 1b) and expressed less Blimp-1–GFP than their wild-type counterparts (Fig. 1c, left). However, lung-infiltrating (Fig. 1c, right) and splenic antigen-specific SLECs had high Blimp-1 expression even in the absence of IL-2 signals (Supplementary Fig. 1c). Stimulation of preactivated IL-2Rα–deficient $CD8^+$ T cells with IL-2 did not result in phosphorylation of transcription factor STAT5, whereas stimulation with IL-15 did, ruling out the possibility that IL-2Rα–deficient $CD8^+$ T cells responded to IL-2 signals via the intermediate affinity receptor IL-2Rβ-γ_c (Supplementary Fig. 1d). Taken together, these results indicate that IL-2 is not essential for the induction of Blimp-1 but is required for its optimal expression.

IL-2–STAT5 and IL-12–STAT4 ‘cooperate’ in Blimp-1 induction

To dissect the effects of individual cytokines on Blimp-1 expression in the absence of autocrine IL-2 signaling during T cell activation, we generated IL-2–deficient (*Il2*$^{-/-}$) *Blimp1*^{GFP} mice. Naive CD8^{+} T cells sorted from spleens and lymph nodes of *Il2*$^{+/+}$*Blimp1*^{GFP} (hereafter *Blimp1*^{GFP}) and *Il2*$^{-/-}$*Blimp1*^{GFP} mice were stimulated with anti-CD3 and anti-CD28 in the presence of cytokines IL-2, IL-12 and IL-6 alone or in various combinations. In the presence of IL-2 alone, Blimp-1–GFP was not upregulated in either *Blimp1*^{GFP} or *Il2*$^{-/-}$*Blimp1*^{GFP} CD8^{+} T cells (Fig. 1d). However, addition of the proinflammatory cytokine IL-12, but not IL-6, together with IL-2 induced Blimp-1–GFP expression in CD8^{+} T cells from both groups (Fig. 1d) but did not alter the number of cell divisions (Supplementary Fig. 1e). Cross-titration of IL-2 and IL-12 revealed that both cytokines potently synergized to induce high expression of Blimp-1–GFP in CD8^{+} T cells (Fig. 1e). In contrast, IL-15 did not induce Blimp-1–GFP in activated CD8^{+} T cells, even in the presence of IL-12 (Supplementary Fig. 1f). Consistent with a role for IL-12 in regulating Blimp-1 expression *in vivo*, antigen-specific *Blimp1*^{GFP} CD8^{+} T cells responding in *Il12*$^{-/-}$ host mice that were infected with lymphocytic choriomeningitis virus (LCMV, strain WE) expressed reduced amounts of Blimp-1–GFP (data not shown).

Both STAT5 and STAT4 can bind to the *Blimp1* gene in activated CD4^{+} T cells[43]. Chromatin immunoprecipitation of CD8^{+} T cells stimulated with IL-2 or IL-12 *in vitro* showed binding of STAT5 and STAT4 to a gamma-activated site (GAS) motif in intron 3 of *Blimp1* (Fig. 1f). Consistent with an important role for inflammatory signals, particularly IL-12, in inducing Blimp-1, a substantial proportion of activated CD8^{+} T cells in the spleen of *Il2*$^{-/-}$*Blimp1*^{GFP} mice expressed Blimp-1 (Fig. 1g). These observations suggest that proinflammatory signals are a major driver of Blimp-1 expression and compensate for the loss of IL-2 signals under conditions of strong inflammation. Indeed, infection of bone marrow–chimeric mice containing a mix of hematopoietic cells from *Blimp1*^{GFP} (Ly5.1^{+}) and *Il2ra*$^{-/-}$ *Blimp1*^{GFP} (Ly5.2^{+}) mice with LCMV, which causes acute systemic infection and inflammation, resulted in the differentiation of antigen-specific KLRG1^{+}CD8^{+} T cells, which were Blimp-1–GFP^{hi} in both the *Il2ra*$^{-/-}$*Blimp1*^{GFP} and *Blimp1*^{GFP} T cell compartments (Fig. 1h,i). These results suggest that multiple cytokine signals, and IL-2 and IL-12 in particular, act together to overcome a molecular ‘threshold’ required for the expression of high amounts of Blimp-1 and the differentiation of SLECs.

IL-2 regulates SLEC formation in a Blimp-1–dependent manner

To determine which effects of IL-2R signaling are Blimp-1 dependent during effector T cell differentiation, we generated three sets of mixed bone marrow–chimeric mice containing congenically marked hematopoietic cells from wild-type (Ly5.1^{+}) mice mixed with hematopoietic cells from either IL-2Rα–deficient mice, mice lacking Blimp-1 specifically in T cells (expressing *loxP*-flanked *Blimp1* and *Lck*-driven Cre recombinase (*Blimp1*$^{fl/fl}$*Lck*-Cre)) or *Il2ra*$^{-/-}$*Blimp1*$^{fl/fl}$*Lck*-Cre mice (all Ly5.2^{+}). After influenza virus infection, we observed a reduction in antigen-specific CD8^{+} T cells among IL-2Rα–deficient, but not Blimp-1–deficient, CD8^{+} T cells compared to wild-type CD8^{+} T cells (Fig. 2a,b and Supplementary Fig. 2a). Double deficiency of IL-2Rα and Blimp-1 in virus-specific CD8^{+} T cells did not further reduce the numbers of antigen-specific CD8^{+} T cells (Fig. 2a,b and

Supplementary Fig. 2a) indicating that IL-2 mediates expansion of antigen-specific cells independently of Blimp-1. The frequency of antigen-specific KLRG1^{+}IL-7R^{-} SLECs was lower in IL-2Rα–deficient CD8^{+} T cells than in wild-type CD8^{+} T cells and was further reduced in Blimp-1–deficient and IL-2Rα–Blimp-1 double-deficient CD8^{+} T cells, with or without prior priming with heterologous influenza virus (Fig. 2c). In line with this observation, granzyme B (Gzmb) expression was lower in IL-2Rα–deficient, Blimp-1–deficient and double-deficient antigen-specific effector CD8^{+} T cells than in wild-type CD8^{+} T cells (Fig. 2d and Supplementary Fig. 2b). Together, these data indicate that IL-2 signals regulate SLEC differentiation in a Blimp-1–dependent manner, whereas the expansion of antigen-specific T cells is regulated by IL-2 independently of Blimp-1.

A transcriptional signature dependent on IL-2 and Blimp-1

To understand globally the extent to which the IL-2–mediated transcriptional program of effector differentiation is dependent on Blimp-1, we isolated wild-type, IL-2R–deficient and Blimp-1–deficient splenic CD8^{+} T cells specific for the influenza nucleoprotein amino acids 366–374 (NP366^{+}) from the mixed bone marrow–chimeric mice described above and generated gene-expression profiles by RNA sequencing (RNA-seq). More than 50% of the genes differentially expressed between wild-type and Blimp-1–deficient antigen-specific CD8^{+} T cells were also differentially expressed between wild-type and IL-2Rα–deficient cells (Fig. 3a). Most of these genes were associated with effector (*Klrg1*, *Gzma*, *Gzmb*, *Gzmc*, *Serpinb1a*, *Fasl* and *Ctse*), memory T cell differentiation (*Id3*, *Tcf7*) and chemotaxis and adhesion (*Sell*, *Ccr7*, *Cx3cr1* and *Cxcr6*). However, IL-2Rα–deficient CD8^{+} T cells showed deregulated expression of a large number of genes (748) that were Blimp-1 independent—i.e., they were not deregulated in Blimp-1–deficient CD8^{+} T cells. MetaCore analysis showed that these genes are involved in the control of T cell activation, migration and adhesion, cell cycle and inflammation (Fig. 3b). Transcripts that were IL-2 signaling independent—i.e., transcripts deregulated in Blimp-1–deficient but not in IL-2Rα–deficient CD8^{+} T cells—were enriched for genes related to growth arrest and apoptosis (Fig. 3b).

Gene-set enrichment analysis using published MPC and SLEC gene-expression signatures[5] revealed that Blimp-1–dependent genes—i.e., those upregulated in Blimp-1–deficient CD8^{+} T cells or commonly upregulated in Blimp-1–deficient and IL-2Rα–deficient CD8^{+} T cells in comparison to wild-type CD8^{+} T cells—were enriched for MPC signature genes (Fig. 3c). Conversely, transcripts downregulated in both comparisons were enriched for SLEC signature genes (Fig. 3c). Similarly, Blimp–independent genes, upregulated in IL-2Rα–deficient but not in Blimp-1–deficient CD8^{+} T cells, were enriched for MPC signature genes (Fig. 3c). In contrast, genes that were specifically downregulated in IL-2Rα–deficient CD8^{+} T cells were not enriched in the MPC or SLEC signatures (Fig. 3c), suggesting roles in both biological processes distinct from Blimp-1–mediated differentiation.

We next assessed the enrichment of genes specifically deregulated in IL-2Rα–deficient or Blimp-1–deficient CD8^{+} T cells within the ten clusters of genes dynamically regulated during CD8^{+} T cell responses[10] (Fig. 3d). Cluster VI (‘short-term effector and memory’) was the most enriched, with ~30% of genes shared with the sets of genes deregulated in IL-2Rα–deficient CD8^{+} T cells, in both Blimp-1–dependent and Blimp-1–independent

manners. In contrast, clusters II (‘preparation for cell division’), VIII (‘naive or late effector or memory’) and IX (‘short-term effector or memory’) were specifically enriched for genes deregulated in IL-2Rα–deficient but not Blimp-1–deficient $CD8^+$ T cells (Fig. 3d). Together, these data indicate that IL-2 promotes population expansion and other aspects of T cell biology in a Blimp-1–independent fashion and facilitates effector cell differentiation at least in part in a Blimp-1–dependent manner.

Integration of effector and memory T cell development

To test whether IL-2 and Blimp-1 collaboratively control $CD8^+$ T cell differentiation, we extended our RNA-seq analysis to antigen-specific $CD8^+$ T cells that lack both IL-2Rα and Blimp-1, purified from the influenza-infected mixed chimeric mice described above. We found that the ten clusters of transcripts dynamically regulated during a $CD8^+$ T cell response[10] were further deregulated in IL-2Rα–Blimp-1 double-deficient $CD8^+$ T cells compared to single-deficient cells (Fig. 4a). This included cluster VI (‘short term effector and memory’) and clusters VIII, IX and X, which contain genes involved in effector or memory generation. In addition, sizable proportions of genes in clusters II (‘preparation cell division’), IV (‘naive and late memory’) and VII (‘memory precursor’) were derepressed in IL-2Rα–Blimp-1 double-deficient $CD8^+$ T cells (Fig. 4a). This included transcripts encoding molecules important for T cell biology, such as *Ccr6*, *Ccr7*, *Sell* and *Fas*, as well as key transcriptional regulators of effector and memory $CD8^+$ T cell differentiation such as *Myc*, *Eomes*, *Id3* and *Id2*, some of which we confirmed at the protein level (Fig. 4b–d). In line with this observation, gene-set enrichment analysis confirmed that transcripts specifically deregulated in IL-2Rα–Blimp-1 double-deficient $CD8^+$ T cells were strongly enriched for genes deregulated in the absence of Id2 (ref. [34]; Supplementary Fig. 2c). Overall, these data showed that IL-2 signaling and Blimp-1 have common and distinct transcriptional targets and collaborate in the development of effector and memory $CD8^+$ T cells, in part by controlling the expression of other transcriptional regulators critical for antigen-induced T cell differentiation.

Blimp-1 and T-bet regulate distinct and overlapping gene sets

Our results showed that IL-12 contributes to the expression of Blimp-1, but it is also a strong inducer of T-bet (encoded by *Tbx21*), which, similarly to Blimp-1, is required for SLEC differentiation. Flow cytometric analysis showed that T-bet protein expression was not significantly different between antigen-specific IL-2Rα– or Blimp-1–deficient $CD8^+$ T cells and wild-type cells (Fig. 5a). Likewise, Blimp-1 expression was similar in wild-type and T-bet–deficient antigen-specific $CD8^+$ T cells (Fig. 5b), indicating that T-bet and Blimp-1 in $CD8^+$ T cells are expressed largely independently of each other.

To characterize transcriptional signatures specific or common to either of these factors, we performed RNA-seq analysis of $NP366^+CD8^+$ T cells purified from influenza infected bone marrow chimeric mice containing congenically marked $Tbx21^{-/-}$ and wild-type hematopoietic cells. Consistent with the notion that both Blimp-1 and T-bet contribute to SLEC formation, 82 of the genes deregulated in Blimp-1–deficient $CD8^+$ T cells were also deregulated in T-bet–deficient $CD8^+$ T cells (Fig. 5c). When we compared the lists of genes that were expressed differently in T-bet–deficient and IL-2Rα–Blimp-1 double-deficient

$CD8^+$ T cells (relative to wild-type $CD8^+$ T cells), we found that 166 transcripts were deregulated in both data sets (Fig. 5c). This included transcripts associated with immune cell function, T cell migration, adhesion and killing, such as *Cx3cr1*, *Ccr7*, *S1pr5*, *Klrg1*, *Fasl*, *Gzma* and *Prf1*, as well as transcriptional regulators of memory $CD8^+$ T cell differentiation such as *Eomes*, *Tcf7* and *Id3* (Fig. 5d), all of which may be considered part of the core transcriptional program of SLEC versus MPC differentiation. This result suggested that the T-bet and IL-2Rα–Blimp-1 axes act together to control gene expression. Genes deregulated specifically in T-bet–deficient $CD8^+$ T cells compared to wild-type cells were enriched for T cell activation, migration, cytokine signaling and cytotoxic function, as well as for genes controlling cell cycle (Supplementary Fig. 3a). As expected, a majority of MPC and SLEC signature genes[5] were deregulated in the same direction in both Blimp-1–deficient and T-bet–deficient antigen-specific $CD8^+$ T cells (Fig. 5d). Likewise, comparison of the ten clusters of transcripts dynamically regulated during $CD8^+$ T cell responses[10] showed that T-bet and Blimp-1 commonly regulate a large proportion of genes, in particular in clusters I and VI (Fig. 5e). Many genes, however, were more strongly affected by loss of T-bet (*Tox*, *Klrg1*, *Ifitm10*, *Ccl6*) or Blimp-1 (*Tspan12*, *Sell*, *Cxcr5*, *Nsg2*, *Myc*, *Usp18*), respectively, whereas others were regulated in opposite directions (*Nrp1*, *Ifitm1*, *Ifitm3*, *Pou6f1*) (Fig. 5d and Supplementary Fig. 3b,c). Thus, our data demonstrate that Blimp-1 and T-bet have both overlapping and distinct roles in driving the effector program of $CD8^+$ T cell differentiation.

Cooperation in $CD8^+$ T cell–mediated virus control

Our data suggested that Blimp-1 and T-bet act together during effector differentiation of $CD8^+$ T cells in an at least partially nonredundant fashion. To test this hypothesis, we generated three sets of mixed bone marrow–chimeric mice containing congenically marked wild-type ($Ly5.1^+$) and either *Blimp1*$^{fl/fl}$*Lck*-Cre, T-bet–deficient or T-bet–deficient *Blimp1*$^{fl/fl}$*Lck*-Cre (all $Ly5.2^+$) hematopoietic cells and infected them with LCMV. At the peak of the immune response (day 9), antigen-specific $CD8^+$ T cells of all genotypes were present in similar frequencies (Fig. 6a). However, we observed ‘cooperative’ activities of Blimp-1 and T-bet in the generation of polyfunctional antigen-specific $CD8^+$ T cells. Whereas a large population of wild-type $CD8^+$ T cells expressed both GzmB and interferon-γ (IFN-γ), such double producers were reduced among cells lacking either T-bet or Blimp-1 (by ~2-fold and ~6-fold, respectively) and were largely absent in cells lacking both transcription factors (reduced by ~18-fold) (Fig. 6b). Furthermore, we observed synergistic induction of IL-7R but not of CD62L expression (Fig. 6c,d) in T-bet–Blimp-1 double-deficient antigen-specific $CD8^+$ T cells, suggesting ‘cooperation’ in the suppression of memory fate. Similar results were obtained with influenza infection (Supplementary Fig. 4a,b and data not shown).

LCMV infection of nonchimeric *Blimp1*$^{fl/fl}$*Lck*-Cre and T-bet–deficient mice resulted in significantly less SLEC differentiation than in wild-type mice, and a further reduction in T-bet–deficient *Blimp1*$^{fl/fl}$ *Lck*-Cre mice (Fig. 6e and Supplementary Fig. 5a). We also observed defects in viral clearance at days 8–10 after infection, after infection with both low (300 plaque-forming units (PFU) (Fig. 6f) and high (3,000 PFU) (Supplementary Fig. 5b) doses of LCMV, and this defect was most pronounced in T-bet–deficient *Blimp1*$^{fl/fl}$*Lck*-Cre mice (Fig. 6f and Supplementary Fig. 5b). Compared to wild-type and single-deficient mice,

T-bet–deficient *Blimp1*$^{fl/fl}$*Lck*-Cre mice showed higher spleen weight (Supplementary Fig. 5c) and higher expression of CD25 and PD1 on antigen-specific CD8$^+$ T cells (Fig. 6g and Supplementary Fig. 5d,e). Furthermore, T-bet–deficient *Blimp1*$^{fl/fl}$ *Lck*-Cre mice showed accelerated weight loss and died within 10–11 d of LCMV infection, whereas most of the single-deficient and wild-type mice recovered (Fig. 6h and Supplementary Fig. 5f). Depletion of CD8$^+$ T cells, but not CD4$^+$ T cells, resulted in survival of these mice (Fig. 6i and Supplementary Fig. 5g), which indicates that CD8$^+$ T cells mediated the observed immune pathology. These data demonstrate that although Blimp-1 and T-bet are not required for the expansion of antigen-specific CD8$^+$ T cells, they act together during the differentiation of protective effector CD8$^+$ T cells and prevent CD8$^+$ T cell–mediated immune pathology.

Blimp-1 and T-bet nonredundantly regulate T cell function

To understand the specific and overlapping functions of Blimp-1 and T-bet during CD8$^+$ T cell differentiation in response to viral infection, we sorted antigen-experienced wild-type, Blimp-1–deficient, T-bet–deficient and T-bet–Blimp-1 double-deficient CD8$^+$ T cells from LCMV-infected chimeric mice described above and performed transcriptional profiling by RNA-seq. Many genes important for T cell function were differentially expressed between wild-type and T-bet–Blimp-1 double-deficient CD8$^+$ T cells. This included genes critical for the cytotoxic function of effector CD8$^+$ T cells such as *Gzma*, *Gzmb*, *Gzmk*, *Gzmm*, *Prf1* and *Fasl*, all of which were dramatically reduced in T-bet–Blimp-1 double-deficient CD8$^+$ T cells. Concurrently, genes that are typically not expressed in cytotoxic CD8$^+$ T cells, including T_H17-associated *Rorc*, *Il17*, *IL23r* and *Ccr6*, were strongly upregulated in T-bet–deficient and in double-deficient CD8$^+$ T cells (Fig. 7a). In line with this observation, a large proportion of T-bet–deficient and T-bet–Blimp-1 double-deficient CD8$^+$ T cells expressed IL-17 and RORγt, but not IL-22, which was intrinsic to CD8$^+$ T cells, as indicated by analysis of mixed chimeric mice (Fig. 7b and Supplementary Fig. 5h–j). T-bet–deficient *Blimp1*$^{fl/fl}$*Lck*-Cre mice also showed high serum amounts of inflammatory cytokines including GMCSF, TNF, IL-6 and IL-12, which was associated with a strong increase in neutrophil numbers in the spleen and infiltration of mononuclear cells into the liver (Supplementary Fig. 6a–d).

Further analysis of the RNA-seq results revealed that Blimp-1–deficient CD8$^+$ T cells lacked *Gzmb* and *Gzmc* expression, whereas *Gzmk* and *Gzmm* expression was less impaired or even higher than in wild-type cells (Fig. 7c). In contrast, T-bet–deficient CD8$^+$ T cells in comparison to wild-type cells expressed similar amounts of *Gzmb* and *Gzmc*, but lacked *Gzmm* (Fig. 7c). Finally, *Gzma* expression was much lower in both Blimp-1–deficient and T-bet–deficient CD8$^+$ T cells than in wild-type cells, whereas *Gzmk* and *Prf1* expression was severely reduced only in T-bet–Blimp-1 double-deficient cells (Fig. 7c). These data show widespread ‘cooperation’ of Blimp-1 and T-bet in the regulation of genes important for T cell biology, an idea further supported by the expression pattern of the ten clusters of transcripts dynamically regulated during CD8$^+$ T cell responses[10] (Supplementary Fig. 7). Taken together, these results indicate that T-bet and Blimp-1 cooperatively control differentiation of effector CD8$^+$ T cells by promoting the expression of cytotoxic molecules and repressing the alternate cell fate.

T-bet can partially compensate Blimp-1 function

To directly test whether Blimp-1 and T-bet can compensate for each other during effector T cell differentiation, we transduced congenically marked Blimp-1–deficient $CD8^+$ T cells from P14 TCR-transgenic mice, which harbor a TCR specific for the LCMV glycoprotein amino acids 33–41 (gp33), with either a control or a T-bet–overexpressing retrovirus and adoptively transferred them into wild-type recipient mice that had been infected with LCMV (Armstrong) virus 1 d before transfer. T-bet overexpression rescued KLRG1 expression and lowered the expression of IL-7R and Eomes in both wild-type and Blimp-1–deficient $CD8^+$ T cells (Fig. 8a,b), but some alterations associated with Blimp-1 deficiency, such as the loss of Gzmb or the increased expression of memory markers (Tcf1, CD62L) were not corrected by increased T-bet expression (Fig. 8c,d). These data indicate that T-bet only partially compensates for the loss of Blimp-1 during SLEC differentiation and memory development of $CD8^+$ T cells.

DISCUSSION

Using transcriptional profiling of antigen-specific $CD8^+$ T cells lacking several molecules required for SLEC formation, we here reveal two major pathways of effector differentiation governed by the availability of IL-2 and IL-12 and the transcriptional regulators Blimp-1 and T-bet. These two pathways promote cytotoxic effector T cell differentiation and repress alternate cell fate in a collaborative and partially redundant manner, which ensures preservation of effector function in response to various pathogens and over a broad spectrum of pathophysiological conditions.

The molecular network controlling differentiation of effector and memory $CD8^+$ T cells is complex, and cytokines have a central role in shaping it[11–15]. The critical role of IL-2 in promoting effector T cell differentiation is now accepted[16,17]; however, published results showing that IL-2 was both required and dispensable for effector or memory differentiation[26,44–46] are difficult to reconcile and are probably due to the pleiotropic nature of IL-2. Although IL-2 can induce the expression of Blimp-1 (refs. [17–21]), we found that IL-2 alone was neither necessary nor sufficient for *Blimp1* expression. Rather, inflammatory cytokines, in particular IL-12, in combination with IL-2, were essential for *Blimp1* induction.

Our transcriptional profiling of antigen-specific $CD8^+$ T cells lacking IL-2Rα, Blimp-1 or both revealed broad cooperation in the regulation of genes required for antigen-induced T cell differentiation. IL-2–mediated SLEC differentiation was Blimp-1–dependent, but large numbers of genes dynamically regulated during $CD8^+$ T cell responses[10]—including clusters of transcripts involved in effector cell generation, cell division or the memory state—required both IL-2 signaling and Blimp-1 for their appropriate expression. Notably, we found that IL-2 and Blimp-1 act together in controlling the expression of transcriptional regulators such as Eomes and Id2, which are essential regulators of T cell differentiation and function[28–34]. IL-2 also controlled large numbers of genes in a Blimp-1–independent fashion, including genes involved in T cell activation, cell cycle and survival, suggesting that IL-2 signaling guides effector differentiation in both Blimp-1–dependent and Blimp-1–independent ways.

Inflammatory cytokines, including IL-12, are required for efficient T cell responses. Although the contribution of individual cytokines is context dependent, it is likely that several cytokines are involved and can partially compensate for each other[14,15,47]. In line with ‘promiscuous’ regulation of T cell differentiation, Blimp-1 expression is induced not only by IL-12–STAT4 and IL-2–STAT5 but also by IL-21–STAT3 signals[22,48]. IL-12 is also an inducer of T-bet[5,30], in contrast to IL-2, which is dispensable for T-bet expression in $CD8^+$ T cells[17]. Therefore, IL-2 and multiple inflammatory signals induce distinct but overlapping pathways that intersect at the level of Blimp-1 and control effector differentiation.

Our transcriptional profiling showed that Blimp-1 and T-bet were required for the appropriate expression of a common group of molecules that may be considered the core signature of SLEC differentiation. Consequently, T-bet overexpression was able to rescue SLEC differentiation in Blimp-1–deficient T cells, indicating that both factors act in an additive manner during SLEC formation. Such a complementation mechanism may be important to ensure differentiation under conditions of limiting cytokine availability and may constitute a ‘backup’ to maintain effector cell differentiation and function under different physiological conditions. This idea is supported by our finding that T cells that lack either Blimp-1 or T-bet maintain considerable functionality. However, our data also reveal specific functions for Blimp-1 and T-bet, illustrated by the distinct expression patterns of cytotoxic molecules such as granzymes, several of which we found to be specifically regulated by either Blimp-1 or T-bet. Thus, although T-bet and Blimp-1 act together during acquisition of effector function, there is ‘division of labor’ between them at the level of gene regulation.

The cooperative functions of Blimp-1 and T-bet also extended to the repression of lineage-inappropriate genes during cytotoxic T cell differentiation. Whereas T-bet deficiency alone was sufficient to induce substantial IL-17 production from antigen-specific $CD8^+$ T cells, only the additional loss of Blimp-1 resulted in further derepression of genes associated with a pathological potential of IL-17–producing cells, including *Il23r* and *Ccr6*, and caused $CD8^+$ T cell–mediated pathology, a phenotype reminiscent of T cells lacking both T-bet and Eomes[42].

In summary, our results demonstrate widespread molecular cooperation and redundancy during $CD8^+$ effector T cell differentiation and indicate that multiple transcription factors create a ‘buffered’ molecular network that protects against the loss of individual components. Furthermore, our data suggest the existence of a molecular ‘threshold’ in the differentiation of functionally competent effector T cells, consisting of two interdependent layers: cytokines, including IL-2 and IL-12, and transcription factors, including Blimp-1 and T-bet, that act in a combinatorial manner to promote the differentiation process. In this model, different input signals cooperate in an additive manner to induce a transcriptional program that drives effector differentiation. Through the combination of multiple, partially redundant components in this network, cytotoxic T cell function remains intact even when individual components collapse. Such a ‘fail-safe’ system may have been evolutionarily selected for to ensure robust cytotoxic T cell differentiation and function under various conditions including infections with distinct pathogens or tumor development.

METHODS

Methods and any associated references are available in the online version of the paper.

ONLINE METHODS

Mice

Male and female mice were used in this study, all on a C57BL/6 background. *Il2*$^{-/-}$, *Il2ra*$^{-/-}$, *Il12*$^{-/-}$, *Blimp1*^{GFP}, *Blimp1*$^{fl/fl}$ mice crossed to mice that express Cre recombinase under the control of the *lck* proximal promoter (*Blimp1*$^{fl/fl}$*Lck*-Cre$^{T/+}$, *Blimp1*$^{fl/fl}$*Lck*-Cre), P14/*Blimp1*$^{fl/fl}$*Lck*-Cre and *Tbx21*$^{-/-}$ mice have been described[24,25,49–53]. Mixed bone marrow chimeras were generated by reconstituting lethally irradiated (2 × 550 R) Ly5.1 or Ly5.1 × Ly5.2 (F1) mice with a mixture of Ly5.1 and mutant or control (Ly5.2) bone marrow as indicated. In some experiments we used *Blimp1*^{GFP} mice on a Ly5.1 background. Reconstituted mice were allowed 6–8 weeks to recover. Mice were maintained and used in accordance with the guidelines of the Walter and Eliza Hall Institute Animal Ethics Committee. No samples were excluded form the study, and no randomization was used. Investigators were not blinded to group allocation or genotype.

Infections

Mice were anesthetized with methoxyflurane and inoculated with 104 plaque-forming units (PFU) of the HKx31 (H3N2) influenza A virus. In some experiments mice were first inoculated intraperitoneally (i.p.) with 107 PFU of the heterologous influenza virus A/PR/8/34 (H1N1, PR8, Mt Sinai strain) 4–6 weeks before infection with HKx31. Lymphocytic choriomeningitis virus (LCMV, strain WE) infections were done by intravenous (i.v.) injection of 300 PFU or 3,000 PFU unless otherwise indicated. In some experiments mice were infected with LCMV Armstrong (2 × 10^5 PFU) administered i.p.

T cell depletion

Mice were injected i.p. 7 d and 4 d before LCMV infection with 0.1–0.2 mg antibodies to CD4 (GK1.5) or CD8 (YTS-169) (produced in house) and then once a week with 0.1 mg of antibodies until completion of the experiment.

Bio-Plex cytokine assay

Serum cytokines levels of were quantified using the Bio-Plex Pro Mouse Cytokine Assay (Bio-Rad).

Histology

Histological analysis of the liver was performed by staining with hematoxylin and eosin (H&E) on paraffin-embedded histological sections (4 μm) fixed with 10% formalin.

Antibodies and flow cytometry

Fluorochrome-conjugated antibodies directed against the following antigens were used for analysis by flow cytometry (dilutions and catalog or clone numbers are given in parentheses): CD8+α (1:300, 53-6.7), CD62L (1:800, MEL-14), KLRG1 (1:300, 2F1),

IL-7R (1:100, A7R34), PD1 (1:300, J43), CD25 (1:200), 7D4, Ly6c (1:400, HK1.4), F4/80 (1:300, BM8), Eomes (1:500, Dan11mag) (from eBioscience), T-bet (1:100, 4B10, Santa Cruz); Ly5.1 (A20), Ly5.2 (1:200, 104), CD11b (1:400, Mac1), Ly6g (1:400, 1A8), IFN-γ (1:200, XMG1.2), IL-17A (1:200, TC11-18H10), RORγt (1:400, Q31-378), STAT5-pY694 (1:20, 47) (from BD Pharmingen) and GzmB (1:100, GB12, Invitrogen). Propidium iodide or SytoxBlue (Invitrogen) was used to exclude dead cells. In some experiments CD8+ T cells were enriched before analysis by depletion with antibodies against CD11b (M1/70), F4/80 (F4/80), Ter-119, Gr-1 (RB6-8C5), MHC class II (M5/114), and CD4 (GK1.5) (hybridoma supernatant, generated in house). Phosphorylated STAT5 (phospho-STAT5) intracellular staining was performed using the BD PhosFlow staining kit (BD Pharmingen) according to the manufacturer's protocols.

Tetramers and intracellular cytokine staining

Antigen-specific $CD8^+$ T cells were enumerated by staining with MHC class I ($H\text{-}2D^b$) tetramers in complex with influenza $NP_{366–374}$ (NP366) or LCMV $gp_{33–41}$ (gp33) peptides. *In vitro* restimulation was performed using the same antigen-specific peptides in the presence of GolgiPlug (BD Bioscience) for 5 h. Intracellular staining of cytokines and Gzmb was performed using the BD kit and staining of transcription factor was performed using the FoxP3 staining kit (eBioscience) according to the manufacturers' protocols.

LCMV virus titer assay

Organs were homogenized using the Qiagen TissueLyser, and viral titers were quantified by focus-forming assays using MC57 fibroblast cells as described[54].

Cell culture

For *in vitro* Blimp-1 induction experiments, $CD62L^{hi}CD44^{lo}$ CD8+ T cells were sorted by flow cytometry and cultured using plate bound anti-CD3 (2C11, 5 μg/ml), soluble anti-CD28 (37.51, 2 μg/ml) antibodies (both produced in house) and combinations of human recombinant IL-2 (100 U/ml), mouse IL-12 (5 ng/ml) and mouse IL-6 (20 ng/ml) as specified for 5 d. In some experiments, cultures contained 25 μg/mL of anti-mouse IL-2 monoclonal antibody (supernatant from hybridoma cell line S4B6, WEHI), which blocks the activity of mouse IL-2 *in vitro* but does not recognize human IL-2 (hIL-2) (ref. [55]). For phospho-STAT5 induction, mixed Ly5.1 and IL-2Rα–deficient CD8+ T cells were preactivated using plate bound anti-CD3 (3 μg/ml), soluble anti-CD28 (1 μg/ml) antibodies and either IL-2 (50 U/ml) or IL-15 (20 ng/ml) for 2 d, then rested for 1 d in medium only and restimulated for 15 min with IL-2 (100 U/ml).

Retroviral transduction

Viral supernatants for the retroviral constructs described in these studies were obtained by transfection of 293T cells with the respective retroviral construct and Eco-helper as described[5]. Transfections were performed using XtremeGene 9 (Roche). T-bet–expressing and GFP-MSCV vectors were obtained from L. Glimcher[56]. P14 donor cells were activated *in vitro* using 1 μg/ml αCD3 and αCD28 and 1 d later spin-transduced for 90 min at 34 °C with viral supernatants in the presence of 0.8 mg/ml polybrene. After transduction, 0.5–1 ×

10^5 P14 CD8+ T cells were transferred intravenously to recipient C57BL/6 mice that had been infected 1 d prior with LCMV (Armstrong).

RNA sequencing and bioinformatic analysis

RNA sequencing was performed following an adapted protocol. $NP366^+CD8^+$ T cells were purified by flow cytometric sorting (FACS Aria flow cytometer, BD Biosciences) from day 9 HKx31-infected PR8-primed mixed bone marrow chimeras. Alternatively, antigen-experienced ($CD44^+CD62L^{low}$) wild-type, Blimp-1–, T-bet– or T-bet–Blimp-1 double-deficient $CD8^+$ T cells were isolated from mixed bone marrow chimeras 10 d after infection with LCMV. Total RNA was prepared using the RNeasy Plus Mini Kit (Qiagen) according to the manufacturer's instructions. RNA-seq was carried out on the basis of a published protocol, in which 3,000 bases at the 3′ end of each transcript were sequenced[57]. Samples were sequenced on a Genome Analyzer IIx (Illumina) at the US National Heart Lung and Blood Institute. RNA-seq reads were aligned to the GRCm37/mm9 build of the *Mus musculus* genome using the Subread aligner[58]. Only uniquely mapped reads were retained. Genewise counts were obtained using feature-Counts[59] with NCBI RefSeq build 37.2 mouse gene annotation build. Only reads overlapping with the last 3,000 exonic bases (located at 3′ end) of each gene were counted. Genes were filtered from downstream analysis if they failed to achieve a reads per kilobase of exon length per million mapped reads (RPKM) value of at least 0.5 in at least two libraries. Differential expression analysis was performed using Biconductor R package edgeR[60]. A common dispersion was estimated for all genes to measure the global biological variation. A negative binomial generalized log-linear model was fitted to each gene, and likelihood ratio tests were performed to assess differential expression[60]. Genes were called differentially expressed if they achieved a false discovery rate (FDR) of 0.1 or less and also had at least 8 RPKMs in one or both of the two cell types being compared. Gene-set enrichment analysis was carried out using ROAST[61]. Barcode plots were generated using barcodeplot function of the limma package[62]. Heat maps were generated using the gplots package. Biological processes analysis was performed using Metacore (Thomson Reuters) bioinformatics analysis tool.

Microarray analysis

$Id2^{fl/fl}Lck^{Cre}$ Illumina BeadChip data from Masson *et al.*[34] was downloaded from Gene Expression Omnibus (GEO GSE44141). BeadChips were background corrected and normalized using neqc[63]. Probes that failed to achieve a detection P value of <0.05 in at least three arrays were filtered as unexpressed. MPC and SLEC Affymetrix GeneChip data from Joshi *et al.*[5] was downloaded from GEO (GEO GSE8678). GeneChips were background corrected, normalized and summarized using the RMA method. Linear models were fitted to genes and empirical Bayes moderated t-statistic was used to assess differential expression[64] in the analysis of both data sets. A FDR cutoff of 0.05 was applied for calling differentially expressed genes. Gene-set enrichment analysis was conducted using ROAST. All the analysis was carried out using Bioconductor R package limma[62].

Chromatin immunoprecipitation

Wild-type $CD8^+$ T cells were preactivated using plate-bound anti-CD3 (3 μg/ml), soluble anti-CD28 (1 μg/ml) and IL-2 (50 U/ml) for 2 d then rested overnight in medium only. Cells

were restimulated for 1 h with IL-2 (100 U/ml) for STAT5, IL-12 (10 ng/ml) for STAT4 or medium as a control. Cross-linking was done by addition of 1% PFA at room temperature for 10 min, followed by sonication and immunoprecipitation with anti-STAT5A, anti-STAT4 and a corresponding rabbit polyclonal-IgG control (Santa Cruz Technologies). The precipitated DNA was quantified by real-time PCR analysis with SYBR green, which was carried out on a MyiQ instrument (Bio-Rad). Primer sequences were Blimp-1–Stat4/5 forward, TGACTTTCACGACATCCAAGG; Blimp-1–Stat4/5 revers, GGTGTGCCGATCCCAGTAG.

Supplementary Material

Refer to Web version on PubMed Central for supplementary material.

Acknowledgments

We thank M. Camilleri and L. Mackiewicz for technical support, and M. Ghisi (Peter MacCallum Cancer Centre) for assistance with MetaCore bioinformatics analysis. Supported by the National Health and Medical Research Council of Australia (program grant 1054618 to T.P.S. and G.K.S.; fellowship 1058892 to G.K.S.; project grant 1023454 to G.K.S. and W.S.; project grant 637345 to A.K. and G.T.B.; project grant 1042582 to G.T.B. and M.P.; project grant 603122 to M.E.), the Sylvia and Charles Viertel Foundation (A.K. and G.T.B.), the Australian Research Council (S.L.N., G.T.B. and A.K.), the US National Institutes of Health (NIH) (R01AI066232 and R0O1AI074699 to S.M.K.), the Howard Hughes Medical Institute (S.M.K.), the Howard Hughes Medical Institute International Student Fellowship (T.G.), the Division of Intramural Research and the DNA Sequencing Core, National Heart, Lung, and Blood Institute, NIH (W.J.L.), the Adam J. Berry Memorial Fund, jointly provided by the Australian Academy of Science and NIH (A.X.) and the Victorian State Government Operational Infrastructure Support and Australian Government NHMRC Independent Research Institute Infrastructure Support scheme.

References

1. Belz GT, Kallies A. Effector and memory CD8+ T cell differentiation: toward a molecular understanding of fate determination. Curr Opin Immunol. 2010; 22:279–285. [PubMed: 20434894]
2. Kaech SM, Cui W. Transcriptional control of effector and memory CD8+ T cell differentiation. Nat Rev Immunol. 2012; 12:749–761. [PubMed: 23080391]
3. Chang JT, Wherry EJ, Goldrath AW. Molecular regulation of effector and memory T cell differentiation. Nat Immunol. 2014; 15:1104–1115. [PubMed: 25396352]
4. Kaech SM, et al. Selective expression of the interleukin 7 receptor identifies effector CD8 T cells that give rise to long-lived memory cells. Nat Immunol. 2003; 4:1191–1198. [PubMed: 14625547]
5. Joshi NS, et al. Inflammation directs memory precursor and short-lived effector CD8+ T cell fates via the graded expression of T-bet transcription factor. Immunity. 2007; 27:281–295. [PubMed: 17723218]
6. Doering TA, et al. Network analysis reveals centrally connected genes and pathways involved in CD8+ T cell exhaustion versus memory. Immunity. 2012; 37:1130–1144. [PubMed: 23159438]
7. Zehn D, Lee SY, Bevan MJ. Complete but curtailed T-cell response to very low-affinity antigen. Nature. 2009; 458:211–214. [PubMed: 19182777]
8. Man K, et al. The transcription factor IRF4 is essential for TCR affinity-mediated metabolic programming and clonal expansion of T cells. Nat Immunol. 2013; 14:1155–1165. [PubMed: 24056747]
9. Russ BE, et al. Distinct epigenetic signatures delineate transcriptional programs during virus-specific CD8+ T cell differentiation. Immunity. 2014; 41:853–865. [PubMed: 25517617]
10. Best JA, et al. Immunological Genome Project Consortium. Transcriptional insights into the CD8+ T cell response to infection and memory T cell formation. Nat Immunol. 2013; 14:404–412. [PubMed: 23396170]
11. Badovinac VP, Porter BB, Harty JT. CD8+ T cell contraction is controlled by early inflammation. Nat Immunol. 2004; 5:809–817. [PubMed: 15247915]

12. Surh CD, Boyman O, Purton JF, Sprent J. Homeostasis of memory T cells. Immunol Rev. 2006; 211:154–163. [PubMed: 16824125]
13. Rochman Y, Spolski R, Leonard WJ. New insights into the regulation of T cells by γ_C family cytokines. Nat Rev Immunol. 2009; 9:480–490. [PubMed: 19543225]
14. Curtsinger JM, Mescher MF. Inflammatory cytokines as a third signal for T cell activation. Curr Opin Immunol. 2010; 22:333–340. [PubMed: 20363604]
15. Kim MT, Harty JT. Impact of Inflammatory Cytokines on Effector and Memory CD8+ T Cells. Front Immunol. 2014; 5:295. [PubMed: 24995011]
16. Kalia V, et al. Prolonged interleukin-2Rα expression on virus-specific CD8+ T cells favors terminal-effector differentiation *in vivo*. Immunity. 2010; 32:91–103. [PubMed: 20096608]
17. Pipkin ME, et al. Interleukin-2 and inflammation induce distinct transcriptional programs that promote the differentiation of effector cytolytic T cells. Immunity. 2010; 32:79–90. [PubMed: 20096607]
18. Santer-Nanan B, et al. Blimp-1 is expressed in human and mouse T cell subsets and leads to loss of IL-2 production and to defective proliferation. Signal Transduct. 2006; 6:268–279.
19. Gong D, Malek TR. Cytokine-dependent Blimp-1 expression in activated T cells inhibits IL-2 production. J Immunol. 2007; 178:242–252. [PubMed: 17182561]
20. Johnston RJ, et al. Bcl6 and Blimp-1 are reciprocal and antagonistic regulators of T follicular helper cell differentiation. Science. 2009; 325:1006–1010. [PubMed: 19608860]
21. Boulet S, Daudelin JF, Labrecque N. IL-2 induction of Blimp-1 is a key *in vivo* signal for CD8+ short-lived effector T cell differentiation. J Immunol. 2014; 193:1847–1854. [PubMed: 25015830]
22. Kallies A, et al. Transcriptional repressor Blimp-1 is essential for T cell homeostasis and self-tolerance. Nat Immunol. 2006; 7:466–474. [PubMed: 16565720]
23. Kallies A, Nutt SL. Terminal differentiation of lymphocytes depends on Blimp-1. Curr Opin Immunol. 2007; 19:156–162. [PubMed: 17291741]
24. Kallies A, Xin A, Belz GT, Nutt SL. Blimp-1 transcription factor is required for the differentiation of effector CD8+ T cells and memory responses. Immunity. 2009; 31:283–295. [PubMed: 19664942]
25. Rutishauser RL, et al. Transcriptional repressor Blimp-1 promotes CD8+ T cell terminal differentiation and represses the acquisition of central memory T cell properties. Immunity. 2009; 31:296–308. [PubMed: 19664941]
26. Williams MA, Tyznik AJ, Bevan MJ. Interleukin-2 signals during priming are required for secondary expansion of CD8+ memory T cells. Nature. 2006; 441:890–893. [PubMed: 16778891]
27. Feau S, Arens R, Togher S, Schoenberger SP. Autocrine IL-2 is required for secondary population expansion of CD8+ memory T cells. Nat Immunol. 2011; 12:908–913. [PubMed: 21804558]
28. Intlekofer AM, et al. Effector and memory CD8+ T cell fate coupled by T-bet and eomesodermin. Nat Immunol. 2005; 6:1236–1244. [PubMed: 16273099]
29. Banerjee A, et al. Cutting edge: the transcription factor eomesodermin enables CD8+ T cells to compete for the memory cell niche. J Immunol. 2010; 185:4988–4992. [PubMed: 20935204]
30. Takemoto N, Intlekofer AM, Northrup JT, Wherry EJ, Reiner SL. Cutting Edge: IL-12 inversely regulates T-bet and eomesodermin expression during pathogen-induced CD8+ T cell differentiation. J Immunol. 2006; 177:7515–7519. [PubMed: 17114419]
31. Cannarile MA, et al. Transcriptional regulator Id2 mediates CD8+ T cell immunity. Nat Immunol. 2006; 7:1317–1325. [PubMed: 17086188]
32. Knell J, et al. Id2 influences differentiation of killer cell lectin-like receptor $G1^{hi}$ short-lived CD8+ effector T cells. J Immunol. 2013; 190:1501–1509. [PubMed: 23325888]
33. Yang CY, et al. The transcriptional regulators Id2 and Id3 control the formation of distinct memory CD8+ T cell subsets. Nat Immunol. 2011; 12:1221–1229. [PubMed: 22057289]
34. Masson F, et al. Id2-mediated inhibition of E2A represses memory CD8+ T cell differentiation. J Immunol. 2013; 190:4585–4594. [PubMed: 23536629]
35. Ji Y, et al. Repression of the DNA-binding inhibitor Id3 by Blimp-1 limits the formation of memory CD8+ T cells. Nat Immunol. 2011; 12:1230–1237. [PubMed: 22057288]

36. Ichii H, Sakamoto A, Kuroda Y, Tokuhisa T. Bcl6 acts as an amplifier for the generation and proliferative capacity of central memory CD8+ T cells. J Immunol. 2004; 173:883–891. [PubMed: 15240675]
37. Cui W, Liu Y, Weinstein JS, Craft J, Kaech SM. An interleukin-21-interleukin-10-STAT3 pathway is critical for functional maturation of memory CD8+ T cells. Immunity. 2011; 35:792–805. [PubMed: 22118527]
38. Jeannet G, et al. Essential role of the Wnt pathway effector Tcf-1 for the establishment of functional CD8 T cell memory. Proc Natl Acad Sci USA. 2010; 107:9777–9782. [PubMed: 20457902]
39. Masson F, et al. Id2 represses E2A-mediated activation of IL-10 expression in T cells. Blood. 2014; 123:3420–3428. [PubMed: 24723679]
40. Kallies A, et al. A role for Blimp1 in the transcriptional network controlling natural killer cell maturation. Blood. 2011; 117:1869–1879. [PubMed: 21131593]
41. Intlekofer AM, et al. Requirement for T-bet in the aberrant differentiation of unhelped memory CD8+ T cells. J Exp Med. 2007; 204:2015–2021. [PubMed: 17698591]
42. Intlekofer AM, et al. Anomalous type 17 response to viral infection by CD8+ T cells lacking T-bet and eomesodermin. Science. 2008; 321:408–411. [PubMed: 18635804]
43. Liao W, Lin JX, Wang L, Li P, Leonard WJ. Modulation of cytokine receptors by IL-2 broadly regulates differentiation into helper T cell lineages. Nat Immunol. 2011; 12:551–559. [PubMed: 21516110]
44. Bachmann MF, Wolint P, Walton S, Schwarz K, Oxenius A. Differential role of IL-2R signaling for CD8+ T cell responses in acute and chronic viral infections. Eur J Immunol. 2007; 37:1502–1512. [PubMed: 17492805]
45. Obar JJ, Lefrançois L. Early signals during CD8 T cell priming regulate the generation of central memory cells. J Immunol. 2010; 185:263–272. [PubMed: 20519649]
46. Obar JJ, et al. CD4+ T cell regulation of CD25 expression controls development of short-lived effector CD8+ T cells in primary and secondary responses. Proc Natl Acad Sci USA. 2010; 107:193–198. [PubMed: 19966302]
47. Denton AE, Doherty PC, Turner SJ, La Gruta NL. IL-18, but not IL-12, is required for optimal cytokine production by influenza virus-specific CD8+ T cells. Eur J Immunol. 2007; 37:368–375. [PubMed: 17219365]
48. Kwon H, et al. Analysis of interleukin-21-induced Prdm1 gene regulation reveals functional cooperation of STAT3 and IRF4 transcription factors. Immunity. 2009; 31:941–952. [PubMed: 20064451]
49. Sadlack B, et al. Ulcerative colitis-like disease in mice with a disrupted interleukin-2 gene. Cell. 1993; 75:253–261. [PubMed: 8402910]
50. Willerford DM, et al. Interleukin-2 receptor alpha chain regulates the size and content of the peripheral lymphoid compartment. Immunity. 1995; 3:521–530. [PubMed: 7584142]
51. Kallies A, et al. Plasma cell ontogeny defined by quantitative changes in blimp-1 expression. J Exp Med. 2004; 200:967–977. [PubMed: 15492122]
52. Finotto S, et al. Development of spontaneous airway changes consistent with human asthma in mice lacking T-bet. Science. 2002; 295:336–338. [PubMed: 11786643]
53. Lee PP, et al. A critical role for Dnmt1 and DNA methylation in T cell development, function, and survival. Immunity. 2001; 15:763–774. [PubMed: 11728338]
54. Battegay M, et al. Quantification of lymphocytic choriomeningitis virus with an immunological focus assay in 24- or 96-well plates. J Virol Methods. 1991; 33:191–198. [PubMed: 1939506]
55. Marchingo JM, et al. T cell signaling. Antigen affinity, costimulation, and cytokine inputs sum linearly to amplify T cell expansion. Science. 2014; 346:1123–1127. [PubMed: 25430770]
56. Szabo SJ, et al. A novel transcription factor, T-bet, directs T_H1 lineage commitment. Cell. 2000; 100:655–669. [PubMed: 10761931]
57. Tang F, et al. RNA-Seq analysis to capture the transcriptome landscape of a single cell. Nat Protoc. 2010; 5:516–535. [PubMed: 20203668]

58. Liao Y, Smyth GK, Shi W. The Subread aligner: fast, accurate and scalable read mapping by seed-and-vote. Nucleic Acids Res. 2013; 41:e108. [PubMed: 23558742]

59. Liao Y, Smyth GK, Shi W. featureCounts: an efficient general purpose program for assigning sequence reads to genomic features. Bioinformatics. 2014; 30:923–930. [PubMed: 24227677]

60. McCarthy DJ, Chen Y, Smyth GK. Differential expression analysis of multifactor RNA-Seq experiments with respect to biological variation. Nucleic Acids Res. 2012; 40:4288–4297. [PubMed: 22287627]

61. Wu D, et al. ROAST: rotation gene set tests for complex microarray experiments. Bioinformatics. 2010; 26:2176–2182. [PubMed: 20610611]

62. Ritchie ME, et al. limma powers differential expression analyses for RNA-sequencing and microarray studies. Nucleic Acids Res. 2015; 43:e47. [PubMed: 25605792]

63. Shi W, Oshlack A, Smyth GK. Optimizing the noise versus bias trade-off for Illumina whole genome expression BeadChips. Nucleic Acids Res. 2010; 38:e204. [PubMed: 20929874]

64. Smyth GK. Linear models and empirical Bayes methods for assessing differential expression in microarray experiments. Stat Appl Genet Mol Biol. 2004; 3:1–25.

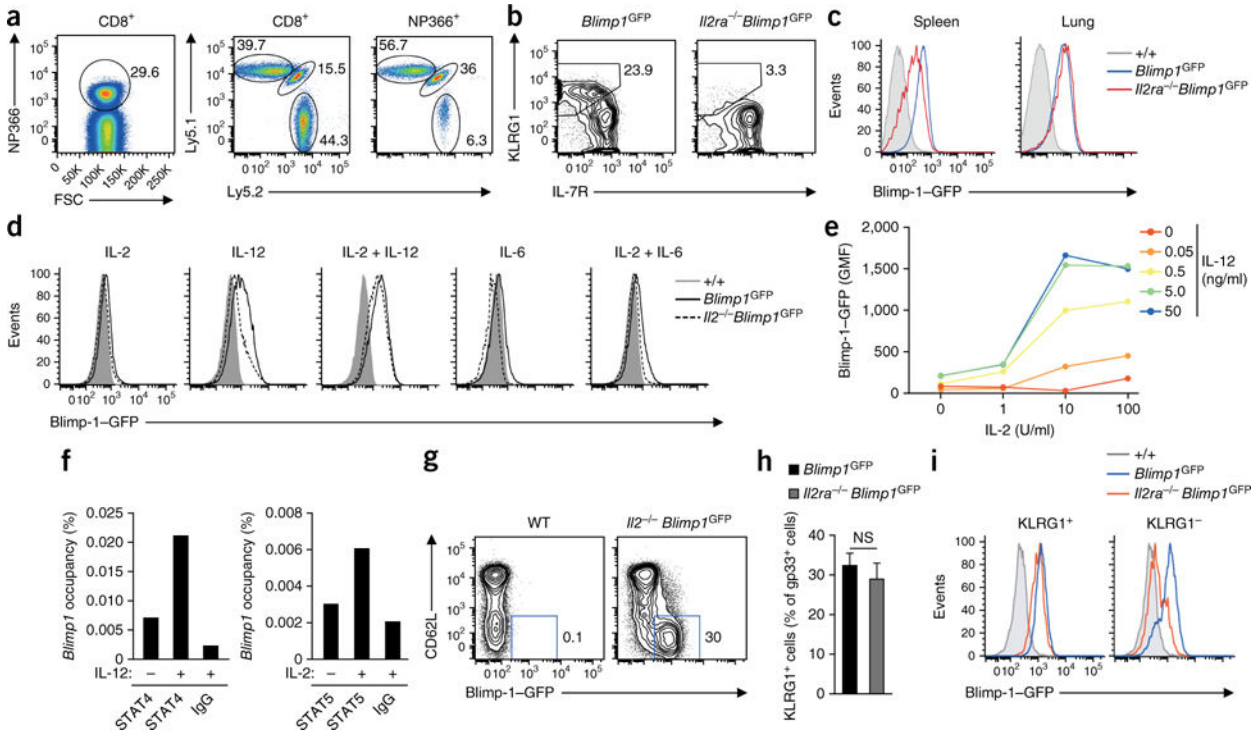

Figure 1.

Inflammation can compensate for IL-2 during Blimp-1 induction. (**a**–**c**) Flow cytometric analysis of splenic CD8$^+$ T cells from irradiated F1 (Ly5.2$^+$Ly5.1$^+$) host mice reconstituted with bone marrow from *Blimp1*^{GFP} (Ly5.1) and *Il12ra*$^{-/-}$*Blimp1*^{GFP} (Ly5.2) mice, primed with PR8 influenza virus and infected 6 weeks later with HKx31 influenza virus, analyzed 9 d after infection. (**a**) Gating strategy for antigen-specific CD8$^+$ T cells. (**b**) Frequency of splenic KLRG1$^+$IL7R$^-$ SLECs. (**c**) Blimp-1–GFP expression in NP366$^+$CD8$^+$ T cells from the spleen or lung. (**d**) Blimp-1–GFP expression in CD8$^+$ T cells from wild-type (+/+), *Blimp1*^{GFP} and *Il2*$^{-/-}$*Blimp1*^{GFP} mice 3 d after activation, cultured with various cytokines. (**e**) Blimp-1–GFP expression of CD8$^+$ T cells cultured in cross-titrated concentrations of human IL-2 and mouse IL-12 in the presence of neutralizing antibody to murine IL-2. GMFI, geometric mean fluorescence intensity. (**f**) Quantification of *Blimp1* gene occupancy by STAT4 (left) and STAT5 (right) in cytokine-stimulated activated CD8$^+$ T cells, as determined by chromatin immunoprecipitation. (**g**) Blimp-1–GFP expression in splenic CD8$^+$ T cells isolated from 6- to 8-week-old wild-type (WT) and *Il2*$^{-/-}$*Blimp1*^{GFP} mice. (**h**) Frequency of KLRG1$^+$ cells in gp33$^+$CD8$^+$ T cells from chimeric mice generated as in **a** on day 8 after infection with LCMV. (**i**) Blimp-1–GFP expression in KLRG1$^+$ and KLRG1$^-$ gp33$^+$CD8$^+$ T cells. NS, not significant (Mann-Whitney *U*-test). Data are representative of one out of two (**e**,**f**, mean of experimental duplicates) or three experiments (**d**), or are representative (**a**–**c**,**g**,**i**) or cumulative (**h**, mean ± s.e.m.) of three experiments, each with n = 3–5 mice per group. Outlined areas in flow cytometric plots and adjacent numbers represent percentages.

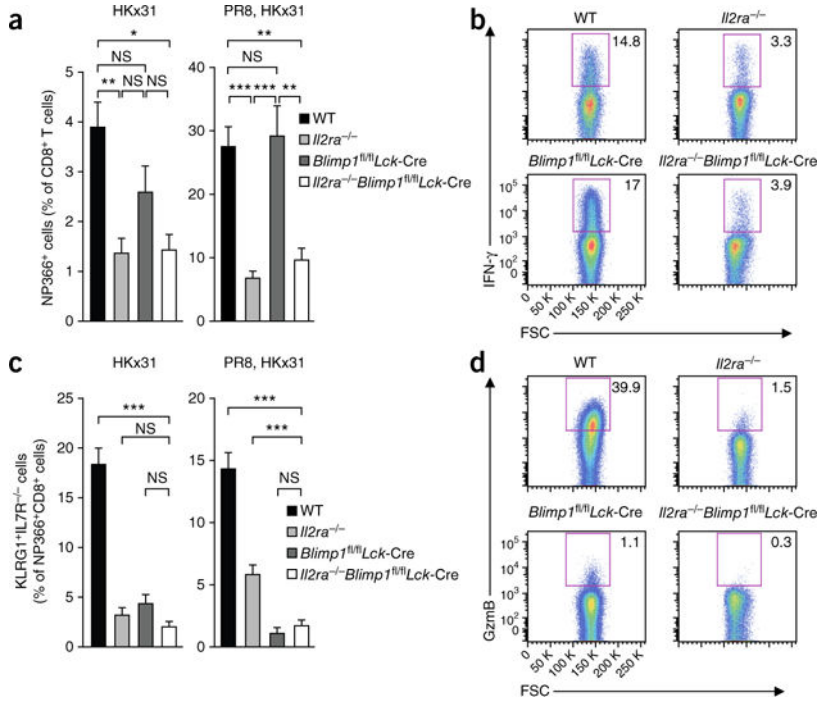

Figure 2.

IL-2R signaling regulates SLEC differentiation in a Blimp-1–dependent manner. (**a**) Frequency of NP366^{+} cells in CD8^{+} T cells from irradiated (Ly5.1^{+}) host mice reconstituted with bone marrow from wild-type (WT, Ly5.1^{+}) and *Blimp1*$^{fl/fl}$*Lck*-Cre, *Il2ra*$^{-/-}$, *Il2ra*$^{-/-}$*Blimp1*$^{fl/fl}$*Lck*-Cre or WT mice (all Ly5.2^{+}), analyzed 9–10 d after infection with HKx31 influenza virus, with or without priming with PR8 influenza virus. (**b**) Interferon-γ (IFN-γ) production of CD8^{+} T cells from PR8-primed chimeric mice after restimulation with NP366 peptide, determined by intracellular staining 9 d after HKx31 infection. (**c**) KLRG1 and IL-7R expression on NP366^{+}CD8^{+} T cells in chimeric mice infected as in **a**. (**d**) GzmB production of CD8^{+} T cells from PR8-primed HKx31-infected mixed chimeras stimulated as in **b**. *$P < 0.05$; **$P < 0.005$; ***$P < 0.001$; NS, not significant (Mann-Whitney *U*-test). Data are mean ± s.e.m. of three experiments, each with $n = 3$–5 mice per group (**a**,**c**) or are from one experiment representative of three, each with $n = 2$–3 mice per group (**b**,**d**). Outlined areas in flow cytometric plots and adjacent numbers represent percentages.

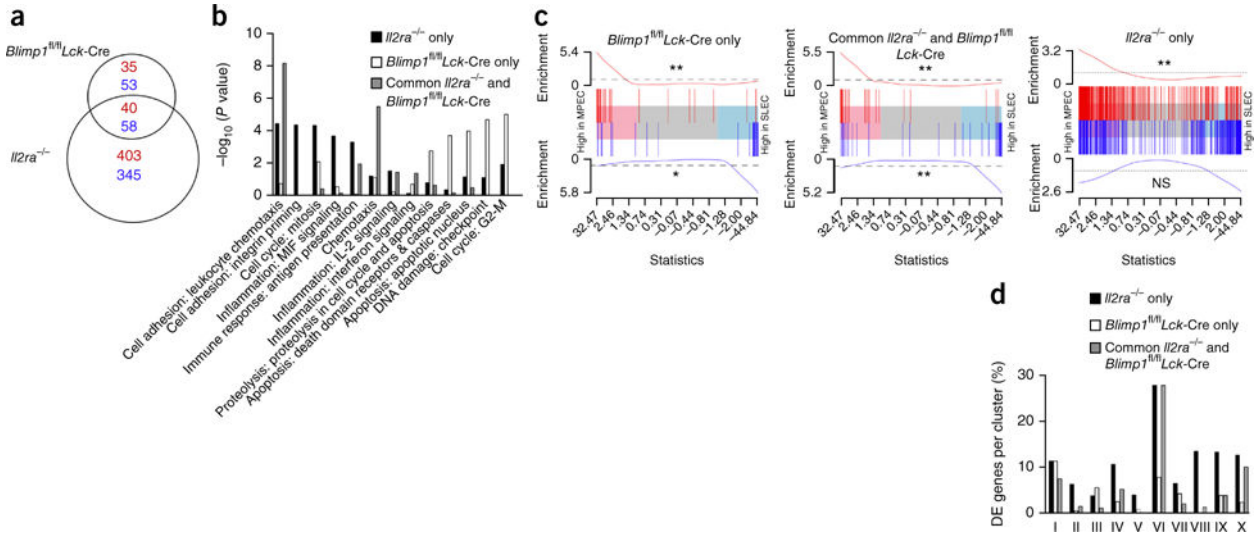

Figure 3.

Blimp-1–dependent and Blimp-1–independent transcriptional signatures induced by IL-2 signaling. (**a**) Whole-genome gene-expression analysis of splenic NP366^{+}CD8^{+} T cells sorted by flow cytometry from mixed bone marrow chimeras as in Figure 2 primed with PR8 and infected with HKx31 influenza virus. Venn diagram shows the overlap of genes expressed differently between antigen-specific Blimp-1–deficient (*Blimp1*$^{fl/fl}$*Lck*-Cre) and IL-2Rα–deficient (*Il2ra*$^{-/-}$) CD8^{+} T cells (red, upregulated; blue, downregulated in comparison to wild-type (WT)). (**b**) MetaCore analysis of biological processes relevant to immune function for genes expressed differently in *Il2ra*$^{-/-}$ CD8^{+} T cells, *Blimp1*$^{fl/fl}$*Lck*-Cre NP366^{+}CD8^{+} T cells or in both *Blimp1*$^{fl/fl}$*Lck*-Cre and *Il2ra*$^{-/-}$ NP366^{+}CD8^{+} T cells. (**c**) Enrichment analysis of indicated gene sets in published MPC and SLEC gene-expression signatures[5]. Graphs show enrichment scores for upregulated (red) and downregulated (blue) genes expressed differently in only *Blimp1*$^{fl/fl}$*Lck*-Cre NP366^{+}CD8^{+} T cells (left), both *Blimp1*$^{fl/fl}$*Lck*-Cre and *Il2ra*$^{-/-}$ NP366^{+}CD8^{+} T cells (middle) or only *Il2ra*$^{-/-}$ NP366^{+}CD8^{+} T cells (right). (**d**) Proportion of genes within each of the ten clusters of genes dynamically regulated during a CD8^{+} T cell response10 that are differentially expressed in *Il2ra*$^{-/-}$ (Blimp-1–independent), *Blimp1*$^{fl/fl}$*Lck*-Cre (IL-2-independent) or both *Blimp1*$^{fl/fl}$*Lck*-Cre and *Il2ra*$^{-/-}$ NP366^{+}CD8^{+} T cells. *$P < 0.01$, **$P < 0.001$; NS, not significant (ROAST test). Data are from RNA-sequencing analysis of two biologically independent samples, each pooled from $n = 5$–6 mice (**a**–**d**).

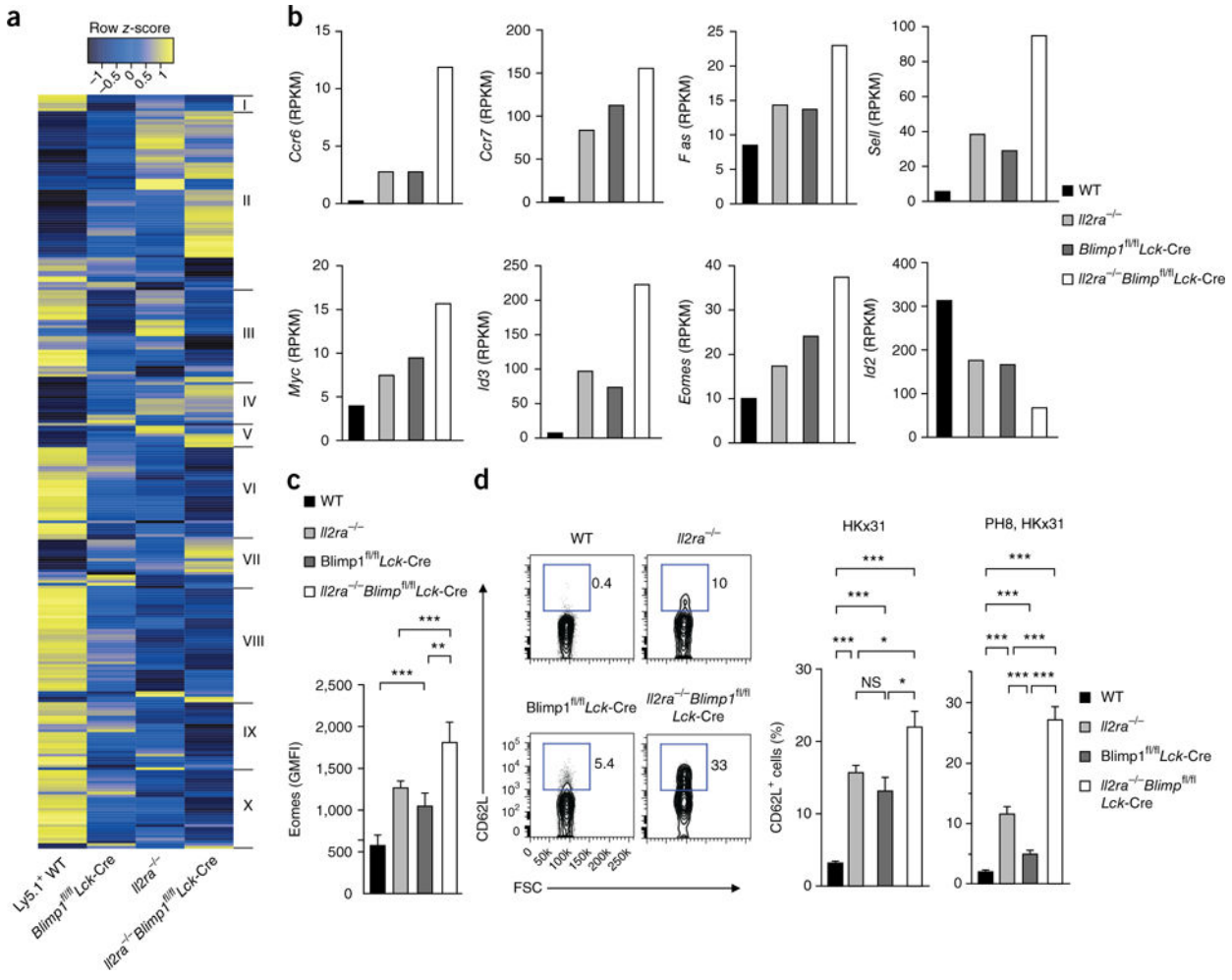

Figure 4.

IL-2Rα and Blimp-1 collaborate in regulating the differentiation of effector CD8$^+$ T cells. (**a**) Whole-genome gene-expression analysis of splenic NP366$^+$CD8$^+$ T cells sorted by flow cytometry from mixed bone marrow chimeras as in Figure 2, primed with PR8 and infected with HKx31 influenza virus. Heat map shows the relative expression level (*z*-score) of deregulated genes identified from RNA-seq analysis of Blimp-1–deficient (*Blimp1*$^{fl/fl}$*Lck*-Cre), IL-2Rα–deficient (*Il2ra*$^{-/-}$) or IL-2Rα–Blimp-1 double-deficient and wild-type (WT) NP366$^+$CD8$^+$ T cells that belong to the ten clusters of genes dynamically regulated during CD8$^+$ T cell responses10. (**b**) Expression in reads per million reads (RPKM) of selected genes in NP366$^+$CD8$^+$ T cells as determined by RNA-seq. (**c**) Geometric mean fluorescence intensity (GMFI) of Eomes expression analyzed by flow cytometry in NP366$^+$CD8$^+$ T cells from PR8-primed chimeric mice 9–10 d after HKx31 infection. (**d**) Flow cytometric analysis (top) and quantification (bottom) of CD62L expression on NP366$^+$CD8$^+$ T cells of various genotypes isolated from mixed chimeric mice that were infected with HKx31 with or without prior PR8-virus priming 9–10 d after infection. Outlined areas in flow cytometric plots and adjacent numbers represent percentages. *$P < 0.01$; **$P < 0.005$; ***$P < 0.001$; NS, not significant (Mann-Whitney *U*-test). Data are from RNA-sequencing of two independent biological samples each pooled from 5–6 mice (**a**,**b**) or are from one experiment

representative of three (**d**, left) or cumulative from (**c**,**d**, right, mean ± s.e.m.) three experiments, each with $n = 3–4$ mice per group.

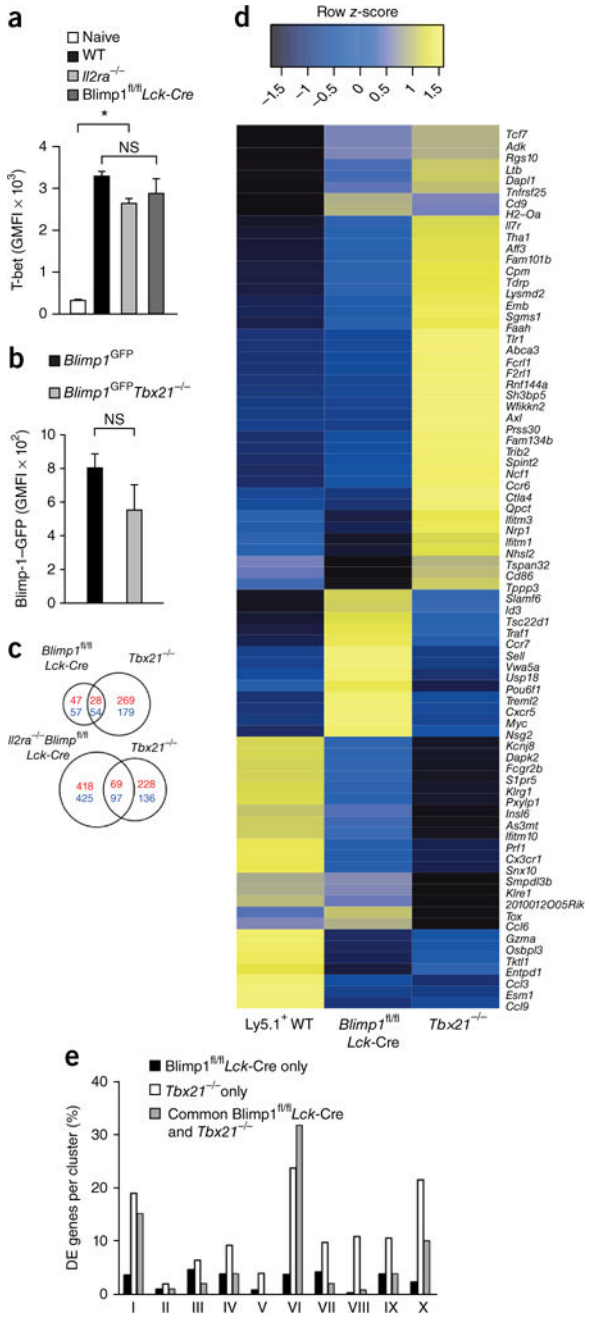

Figure 5.

T-bet and Blimp-1 regulate overlapping and distinct transcriptional signatures during effector CD8$^+$ T cell differentiation. (**a**) Geometric mean fluorescence intensity (GMFI) of T-bet expression analyzed by flow cytometry in NP366$^+$CD8$^+$ T cells from mixed bone marrow–chimeric mice as in Figure 2, after infection with HKx31 influenza virus. (**b**) Blimp-1–GFP expression in NP366$^+$CD8$^+$ T cells of the indicated genotypes in chimeric mice reconstituted with a mix of *Tbx21*$^{-/-}$; *Blimp1*^{GFP} and *Blimp1*^{GFP} bone marrow 9 d after infection with HKx31. (**c**) Comparison of differentially expressed (DE) genes identified by RNA-seq analysis of NP366$^+$CD8$^+$ T cells of various genotypes sorted from mixed

chimeric mice that were primed with PR8 and infected with HKx31. Venn diagrams show the overlap of DE genes in $NP366^{+}CD8^{+}$ T cells in each genotype (red, upregulated; blue, downregulated in comparison to wild-type). (**d**) Heat map showing relative expression levels (*z*-score) of DE genes that are part of published MPC and SLEC gene-expression signatures5. (**e**) Percentages of genes within each of the ten clusters dynamically regulated during a $CD8^{+}$ T cell response[10] that are DE specifically in T-bet–deficient or Blimp-1–deficient $NP366^{+}CD8^{+}$ T cells or shared between the groups. $*P < 0.001$ (Mann-Whitney *U*-test in **a**); NS, not significant (paired *t*-test in **b**). Data are cumulative of two independent experiments, each with 2–3 mice per group (**a**, mean ± s.e.m.), two independent biological samples, each pooled from 5–6 mice (**c**–**e**, mean ± s.e.m.) or one experiment with 5 mice per group (**b**, mean ± s.e.m.).

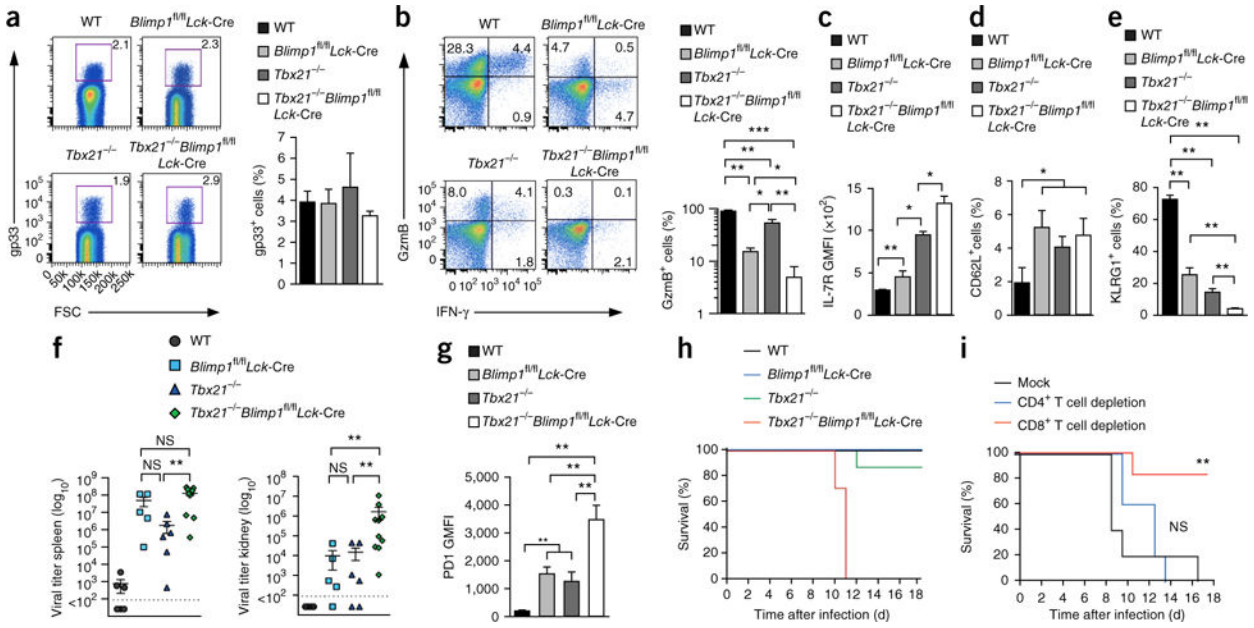

Figure 6.

T-bet and Blimp-1 are required for protective antiviral CD8$^+$ T cell responses. (**a**) Flow cytometric analysis of gp33$^+$CD8$^+$ T cells (left) and quantitative data (right) from splenic CD8$^+$ T cells from chimeric mice reconstituted with a mix of wild-type (WT, Ly5.1$^+$) and *Tbx21*$^{-/-}$,*Blimp1*$^{fl/fl}$*Lck*-Cre or *Tbx21*$^{-/-}$*Blimp1*$^{fl/fl}$*Lck*-Cre (Ly5.2$^+$) bone marrow and infected with LCMV 8 d before analysis. (**b**) Flow cytometric analysis of IFN-γ and GzmB in CD8$^+$ T cells as in **a** after restimulation and intracellular staining (left) and frequencies of GzmB$^+$ cells within IFN-γ$^+$CD8$^+$ T cells (right). (**c**,**d**) IL-7R expression (**c**) and CD62L expression (**d**) on gp33$^+$CD8$^+$ T cells as in **a**. GMFI, geometric mean fluorescence intensity. (**e**) Frequency of KLRG1$^+$ cells among gp33$^+$CD8$^+$ T cells from nonchimeric mice infected with LCMV (300 PFU) and analyzed 9–10 d after infection. (**f**) LCMV virus titers in spleens (left) and kidneys (right) from mice as in **e**. (**g**) PD1 expression of gp33$^+$CD8$^+$ T cells as in **e**. (**h**) Survival curves for mice infected as in **e**. (**i**) Survival of *Tbx21*$^{-/-}$*Blimp1*$^{fl/fl}$*Lck*-Cre mice after depletion of CD8$^+$ or CD4$^+$ T cells and LCMV infection (300 PFU). **P* < 0.05; ***P* < 0.01; ****P* < 0.001 in **b**–**g** (Mann-Whitney *U*-test); ***P* = 0.0026 in **i** (log-rank (Mantel-Cox) test); NS, not significant. Data are representative (**a**,**b**, left) or cumulative (**a**,**b**, right and **c**,**d**) of two experiments, each with *n* = 2–5 mice per group (mean ± s.e.m.) or are cumulative from two experiments, each with *n* = 2–4 mice per group (**e**–**g**, mean ± s.e.m.), *n* = 3–4 mice per group (**h**) or *n* = 2–3 mice per group (**i**). Outlined areas in flow cytometric plots and adjacent numbers represent percentages.

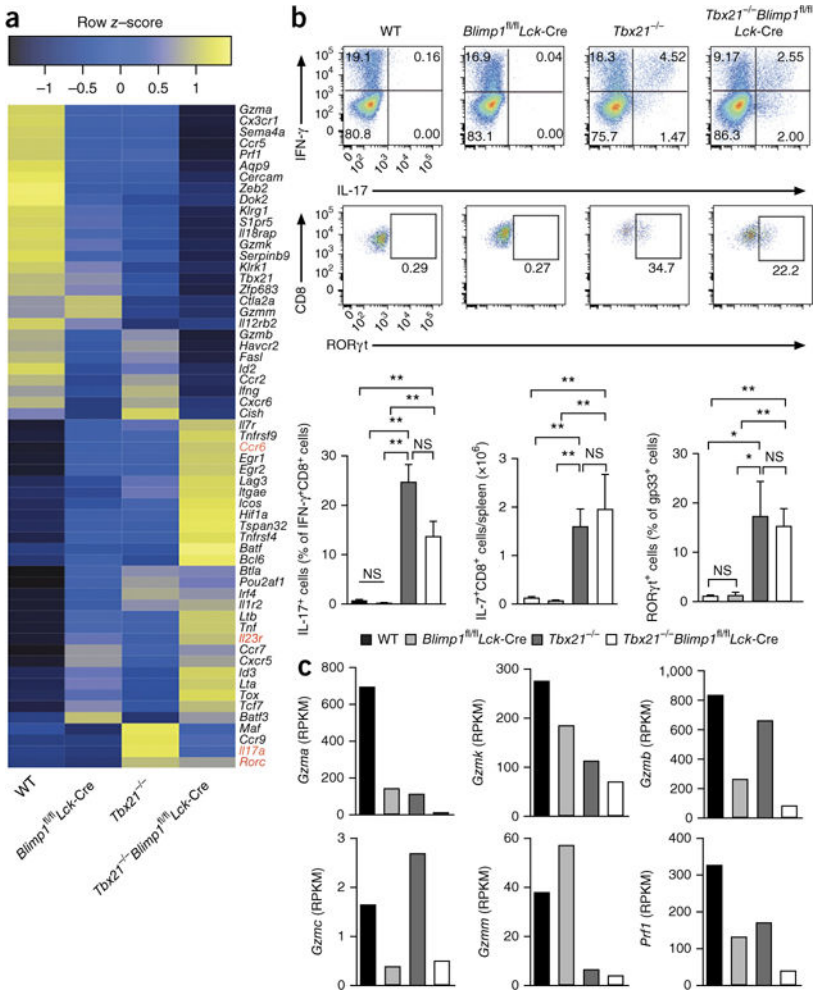

Figure 7.

T-bet and Blimp-1 cooperate during CD8$^+$ T cell effector differentiation and prevent aberrant differentiation of IL-17–producing CD8$^+$ T cells in response to viral infection. (**a**) RNA-seq analysis of antigen-experienced (CD44$^+$CD62L^{lo}) CD8$^+$ T cells from mixed bone marrow chimeric mice, infected with 300 PFU LCMV and analyzed 10 d after infection. Heat map showing relative expression levels (*z*-score) of selected differentially expressed (DE) genes relevant for effector and memory CD8$^+$ T cell differentiation and functions. (**b**) Top, flow cytometric analysis of IFN-γ and IL-17A production by splenic CD8$^+$ T cells from wild-type (WT), *Tbx21*$^{-/-}$, *Blimp1*$^{fl/fl}$*Lck*-Cre or *Tbx21*$^{-/-}$*Blimp1*$^{fl/fl}$*Lck*-Cre mice 9–10 d after infection with LCMV, after restimulation with gp33 peptide and intracellular staining. Bottom, frequencies of IL-17A$^+$ cells in IFNγ$^+$CD8$^+$ T cells (left), absolute numbers of IL17$^+$CD8$^+$ T cells per spleen (middle) and frequencies of RORγt$^+$ cells within gp33$^+$CD8$^+$ T cells (right). Outlined areas in flow cytometric plots and adjacent numbers represent percentages. (**c**) Expression in reads per millions reads (RPKM) of selected genes in antigen-experienced CD8$^+$ T cells of various genotypes from mixed chimeras infected as in **a**, as determined by RNA-seq. **P* < 0.05; ***P* < 0.01; NS, not significant (Mann-Whitney *U*-test). Data are from one experiment representative of two, each with *n* = 2–4 mice per group (**b**, top) or cumulative from two experiments with 2–4 mice per group (**b**, bottom,

mean ± s.e.m.). Data in **a** and **c** are from RNA-sequencing analysis of two biologically independent samples, each pooled from $n = 2$ mice.

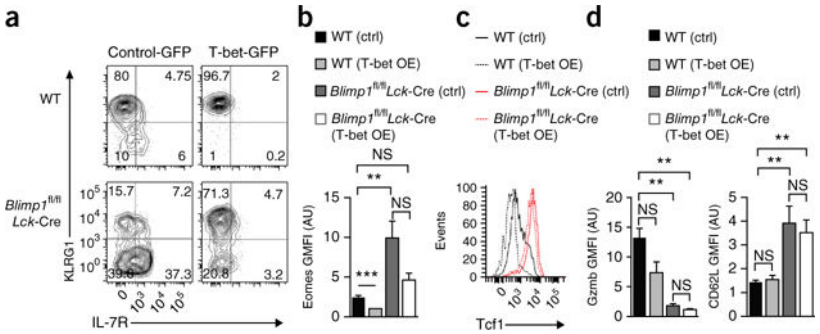

Figure 8.

T-bet can partially compensate for the loss of Blimp-1 in SLEC differentiation. (**a**–**d**) Congenically marked wild-type (WT) or Blimp-1–deficient (*Blimp1*$^{fl/fl}$*Lck*-Cre) P14 TCR transgenic CD8$^+$ T cells transduced with either a T-bet–overexpressing (OE) or control (ctrl) retrovirus were adoptively transferred into recipient mice infected with LCMV (Armstrong) virus the prior day. Donor P14 CD8$^+$ T cells were analyzed by flow cytometry 7 d later. (**a**) KLRG1 and IL-7R expression in WT and Blimp-1–deficient CD8$^+$ T cells transduced with retroviruses as indicated. Outlined areas in flow cytometric plots and adjacent numbers represent percentages. (**b**) Quantification of Eomes expression in CD8$^+$ T cells as in **a**. Data are shown as geometric mean fluorescence intensity (GMFI) arbitrary units (AU). (**c**) Tcf1 expression in CD8$^+$ T cells as in **a**. (**d**) Gzmb (left) and CD62L expression (right) in CD8$^+$ T cells as in **a**. *$P < 0.05$; **$P < 0.01$; NS, not significant (Mann-Whitney *U*-test). Data are from one representative of two experiments with 2–5 mice per group (**a**,**c**) or are cumulative of two experiments with 2–5 mice per group (**b**,**d**, mean ± s.e.m.).